Agronomy Research **16**(S1), 1085–1094, 2018
https://doi.org/10.15159/AR.18.108

Plantograf V18 – new construction and properties

P. Koder[1], V. Novák[1,*], V. Ryzhenko[1], D. Hrubý[2], J. Volf[1] and D. Novák[3]

[1]Czech University of Life Sciences Prague, Faculty of Engineering, Department of Electrical and Automation, Kamýcká 129, CZ165 21 Prague, Czech Republic
[2]Slovak University of Agriculture in Nitra, Faculty of Engineering, Department of Electrical Engineering, Automation and Informatics, Tr. Andreja Hlinku 2, SK949 76 Nitra, Slovakia
[3]Matej Bel University, Faculty of Natural Sciences, Department of Technology, Tajovského 40, SK974 01 Banská Bystrica, Slovakia
[*]Correspondence: novakviktor@tf.czu.cz

Abstract. The article describes Plantograf V18, a planar tactile transducer, which converts the applied pressure into electric signal and enables a graphical presentation of the measured data; the new version V18 comes with some significant improvements and modifications. The device may be used everywhere where the pressure distribution between an object and surface is to be determined, e.g. in medicine or automotive industry. The article contains the detailed description of the transducer design and its electronic control circuits, as well as the yet unpublished measurements of pressure sensitivity with 3.5 mm electrodes.

Key words: transducer, pressure, sensor, conductive ink, FPGA.

INTRODUCTION

The described device represents a new development of the planar pressure converter Plantograf with some significantly enhanced features. The aim of the measuring system Plantograf is to measure the pressure distribution between an object and the surface; it was originally developed for medical purposes to measure the pressure under human feet; the later versions were also used for industrial applications, e.g. for designing car seats in the automotive industry.

The further development of this measuring system is justified by new requirements, which cannot be fulfilled using the preceding versions. The new development reflects besides other things the needs on the fields of:

- agricultural engineering – to enable to measure the soil compaction, i.e. the pressure within soil mass. The new version should have its own power supply and thus it will be independent on the availability of the power source, ready to use in 'field conditions';
- automotive industry – to enhance the accuracy of the pressure measurement under car tire patterns. The present resolution was insufficient; the new development should enhance both the resolution and the frame rate. This way it will be possible to measure fine pressure distribution under tire patterns, particularly with

dependency on the tire inflation, as well as dynamic processes when driving over a pad. For tractor tire patterns see example in Fig. 1;

- medical science – there were also requirements for improving both the resolution and the frame rate, to capture highly dynamic processes, e.g. athlete training.

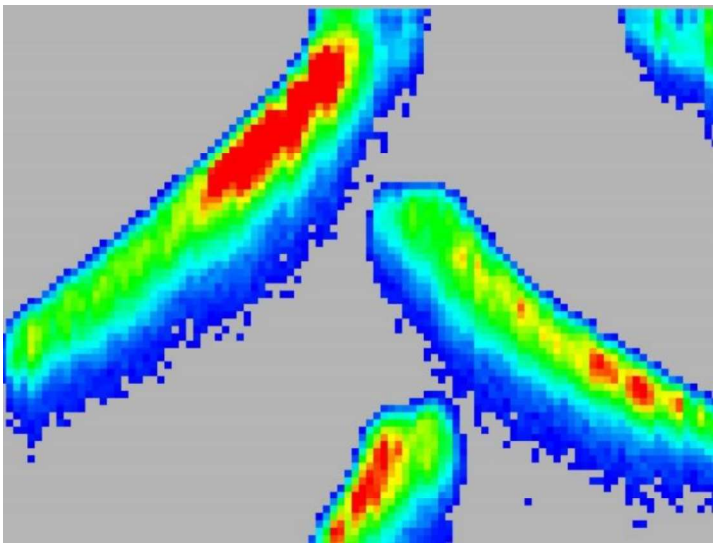

Figure 1. Pressure distribution under tractor tire pattern.

Compared to its predecessors, the new version should be capable with connection with new software and new material, i.e. conductive ink, to measure absolute pressure acting on the transducer, not only relative pressures on 8-bit scale. The main improvements concern the control electronic circuits, which enable to raise both the resolution and the frame rate, up to 500 fps on 128 x 128 matrix. The previous versions also exhibited too low sensitivity, caused by the impossibility of the gain change, which limited the width of measured pressure ranges. This issue will be also corrected with the new version, to extend the operation possibilities of the device. Given the number of 16,400 sensors (on a 500 x 500 mm matrix, 4 mm spacing and 2.5 mm or 3.5 mm electrode diameter) and the expected high scan speed, the described requirements yield some construction improvements and modifications, although the base principle stays the same; for additional information about principles of tactile sensing see Lee (2000); Weiss & Worn (2005); Dahiya & Valle (2008) and Fraden (2010).

Besides the named improvements, the new construction also supports wireless transmission of complete snapshots from the entire sensor. To enhance its 'field use' for measuring of e.g. soil compaction, it also allows battery power unlike its predecessors.

In the first stage, it was necessary to verify the appropriate material that would serve as a transducer between the applied pressure on the sensor and the measured electrical resistance. The main requirement is to measure a significant change of electrical resistance when pressure change occurs within the operating range of the sensor, and secondly that such dependence is linear or at last that it is possible to express by another simple mathematical function.

At this stage, the tried and tested DZT-3K conductive ink was used – for more details see our previous work in Volf et al. (2015) and Volf et al. (2016) – and the sensors were calibrated to verify the correct operation of the control electronics and of the individual sensors itself.

MATERIALS AND METHODS

Sensor overview and construction

From the physical point of view, the device is a transducer between the pressure and the magnitude of the measured electrical resistance, with the pressure being displayed with an 8-bit resolution, i.e. on a scale of 0–255. There are three main parts of the measuring system – a sensor field to capture the acting pressure, control electronic circuits and a connected computer running a service program and displaying the pressure distribution snapshots.

On the sensor field, the acting pressure causes the change of the electrical resistance of the material (here conductive ink DZT-3K), which is measured in real-time by electrical circuits. The calculation of the electrical resistance bases on the principle of a voltage divider, the scheme of which is shown in Fig. 2. The electrical resistance R_{INK} is calculated using the formula:

$$R_{INK} = \frac{R_{CONST} \cdot U_{INK}}{U_{NAP} - U_{INK}} \tag{1}$$

where R_{INK} – calculated electrical resistance of the ink; R_{CONST} – constant electrical resistance 10 kΩ; U_{INK} – measured voltage; U_{NAP} – stabilized supply voltage. The stabilized voltage 2 V is monitored on the output A1+, while the actual measured voltage on the voltage divider (ink layer) is measured on the output A2+, against reference zero (GND).

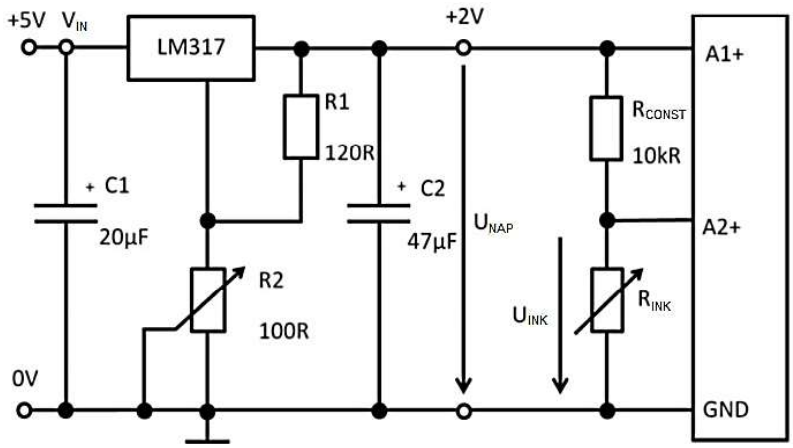

Figure 2. Circuit diagram of the voltage divider.

Fig. 3 shows a section through the entire sensor. The ink is attached to the electrodes on ink carrying layer, which is covered by cover layer that protects the entire sensor from mechanical harm and spreads the pressure on the electrodes. The electrodes

are placed on material called Cuflex that is supported by lower protective layer that protects the sensor from overloading. The passage of the electric current between the electrodes is indicated by a red arrow. The electric current flows from the outer electrode through the conductive ink layer which is deformed and which changes its electrical resistance under the applied pressure into the inner electrode. Further information about conversion of pressure using different materials is in Kim (2009); Astellanos (2010); Seminara (2013) and Volf et al. (2015).

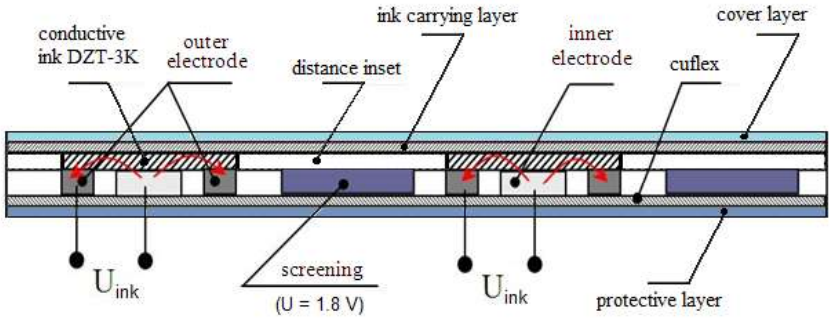

Figure 3. Section through the sensor with indicated current flow.

The new developed sensor matrix consists of individual electrodes with outer diameter of 3.5 mm or 2.5 mm, according to the size of the plate. The electrodes are arranged in an array of 128 x 128 electrodes. A section of the sensor matrix with individual electrodes is shown in Fig. 4.

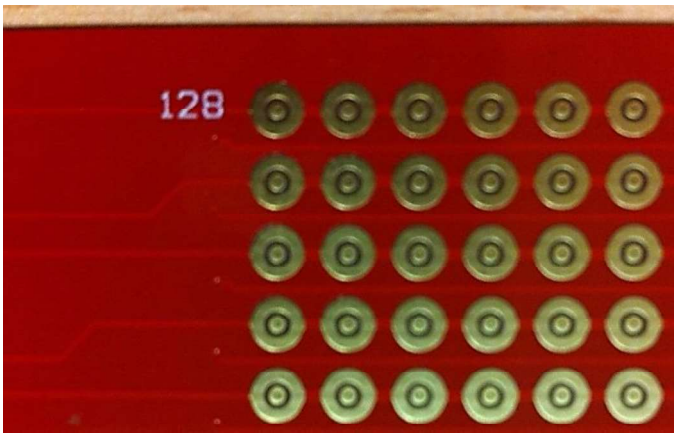

Figure 4. Section of the sensor matrix with individual electrodes.

The control electronics provide measuring of electrical resistance from each sensor of the matrix, which consists of total 16,384 (128 x 128) individual sensors. One image therefore consists of 16,384 scanned points, and given the resolution 8 bits per point (sensor), in represents 131,072 bits for one shot. Considering a frame rate of 500 fps, the processing and data transfer speed reaches up to approximately 8.2 MB/s. The block diagram of the entire system is shown in Fig. 5.

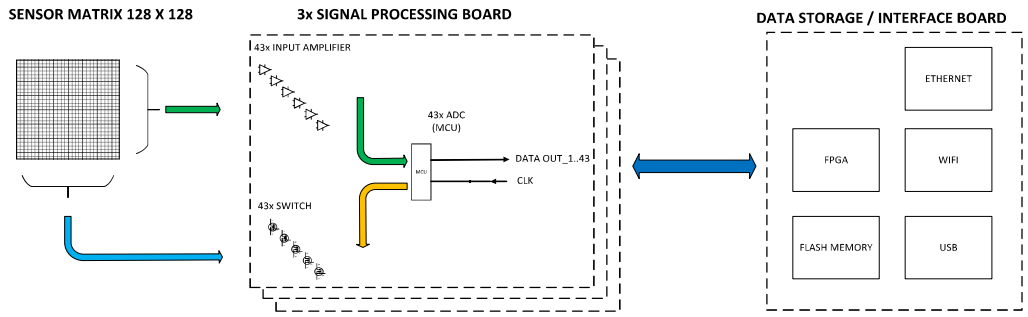

Figure 5. Block diagram of the pressure measuring system Plantograf V18.

The sensor matrix is divided into rows and columns. The columns are connected to voltage and the rows are read. The sensing and converting part of the electronics consists of three identical signal processing modules, each of which contains 43 (up to 45 possible) MOSFET switches that connect the selected column to the power supply. This board also contains 43 amplifiers that measure the sensor's electrical resistance. The signal from them is then led to the appropriate A/D converters. The digitized signal obtained this way is subsequently is fed into the memory and interface board (Field-programmable gate array – FPGA circuit), which provides full control of the Plantograf electronics. It collects the measured data and it provides their further transfer to the computer for further processing and visualization. The communication with the computer runs using USB or Ethernet interface, or wirelessly via Wi-Fi.

Signal processing

The first step in signal processing is provided by 128 (one for each matrix row) individual switches to select a column from the sensor matrix; this is implemented using MOSFET transistors to allow the current from selected column. The raw data is acquired using 128 individual circuits. The resistivity is incorporated into feedback of operating amplifiers, so the output voltage corresponds the resistance and thus the applied pressure onto the sensor. This voltage is led to the A/C conversion.

As the measured resistance of the material represents analogue signal, it has to be converted into digital (8 bit resolution) to allow further computer processing. This is controlled by 128 microprocessors, which also provide the communication with FPGA, set the Q-point of input circuits and control the sequential selection of column matrix. To obtain high sampling frequency, it is necessary to run the digitization parallel on more channels. Every microprocessor is connected with a datalink to superordinate control unit – the FPGA. The microprocessors also control the reference input voltage, to allow the change the Q-point (=working range) of the input circuits. This is used to adjust the measuring range, eliminate errors, calibrating, and for diagnostic purposes. The picture of the electrical control circuits is provided in Fig. 6.

For the function of the whole module, it is necessary to provide different supply voltages, as required by individual electronic circuits. In order to reduce the power loss of the system and the demands on the power supply, switched-mode power supplies are used. The base input supply voltage for the module is 5 V. This voltage is used to power the operational amplifiers and auxiliary sources. Other auxiliary sources provide 3.3 V supply, which is used for powering microprocessors and control logic unit. A negative

voltage of -1.8 V is used to power the amplifiers and as exciting voltage of the columns of the matrix. The supply and electric circuits meet the safety requirements for medical purposes.

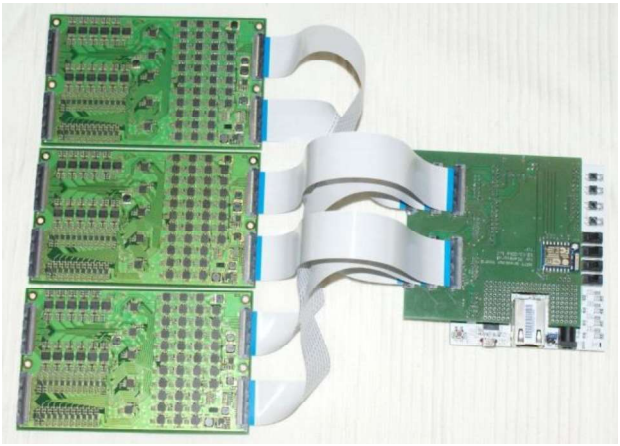

Figure 6. Electrical control unit of Plantograf V18. Three signal processing modules connected to FPGA circuit.

As the main control unit was selected the commercially available FPGA module Xilinx fitted with Artix 7 chip and basic peripherals. This unit also provides communication between the transducer and a connected computer, which runs the service program and displays the snapshots. According to the assignment, the module is besides usual connectivity options additionally fitted with a memory card cap to enable to capture highly dynamic processes as well as with a wireless Wi-Fi module.

RESULTS AND DISCUSSION

The measurement procedure is described in detail in Volf et al. (2016), as the measurement methodology stays the same; here we only summarise the most important facts: given the large number of measurements, the measurement was automatized using Turbo Scara SR60 robot. The applied force was measured by the Hottinger DF2S-3 strain gauge, and the output voltage was captured by the Almemo 2890-9 data logger. Each measurement for a given pressure was performed 10 times, and the measurement uncertainty was calculated from the results.

The testing was carried out on a matrix with 3.5 mm electrodes (outer diameter, labelled OB) placed on a printed board; the board contains conductors drawn from the rows and columns of the matrix, thus enabling the choice of a specific electrode. The following graphs in Figs 7–9 present the dependency of the measured electrical resistance on applied pressure for three ink layers of 6 μm, 17 μm and 26 μm. In the diagrams both the loading cycle and the unloading cycle are depicted and the total (combined) measurement uncertainty is calculated and graphically represented by respective intervals for each measured value.

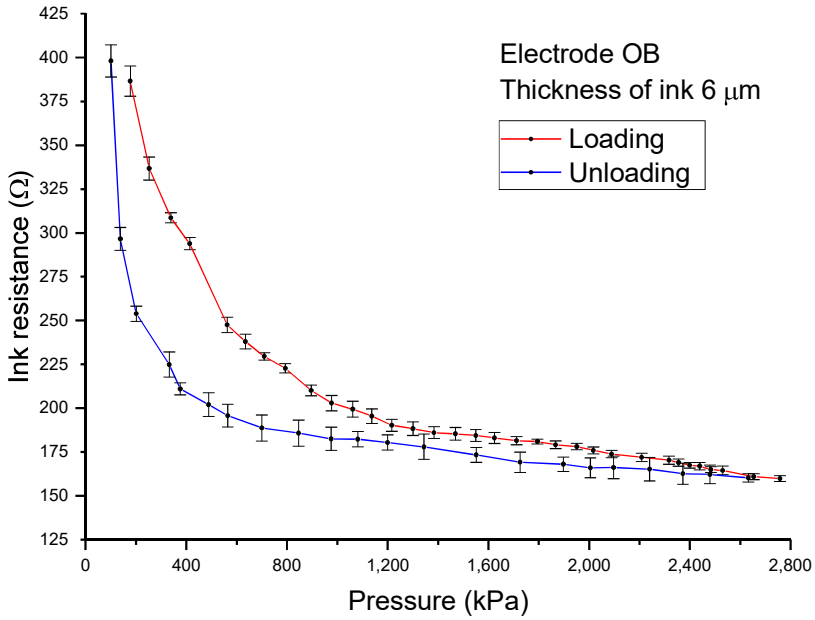

Figure 7. Dependence of measured electrical resistance of a 6 μm thick ink layer on the pressure (loading and unloading cycle).

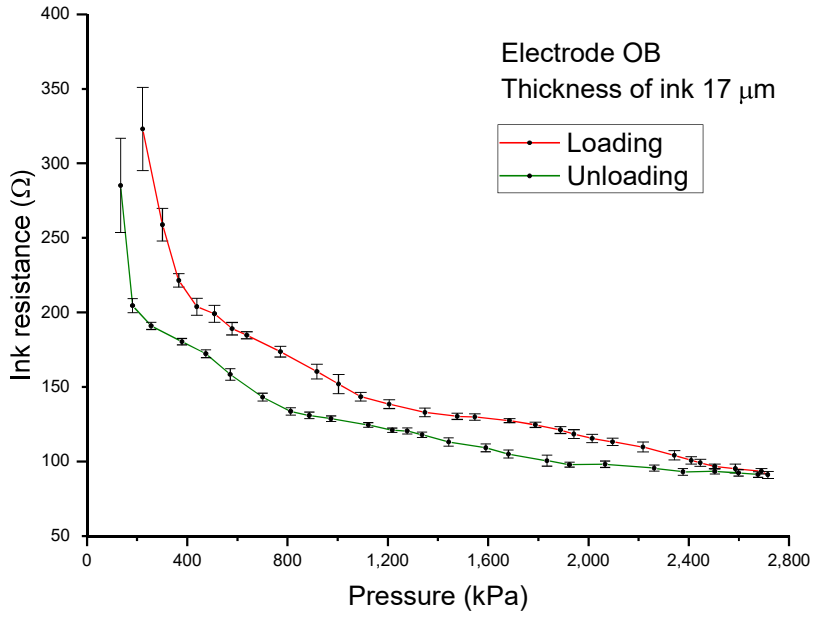

Figure 8. Dependence of measured electrical resistance of a 17 μm thick ink layer on the pressure (loading and unloading cycle).

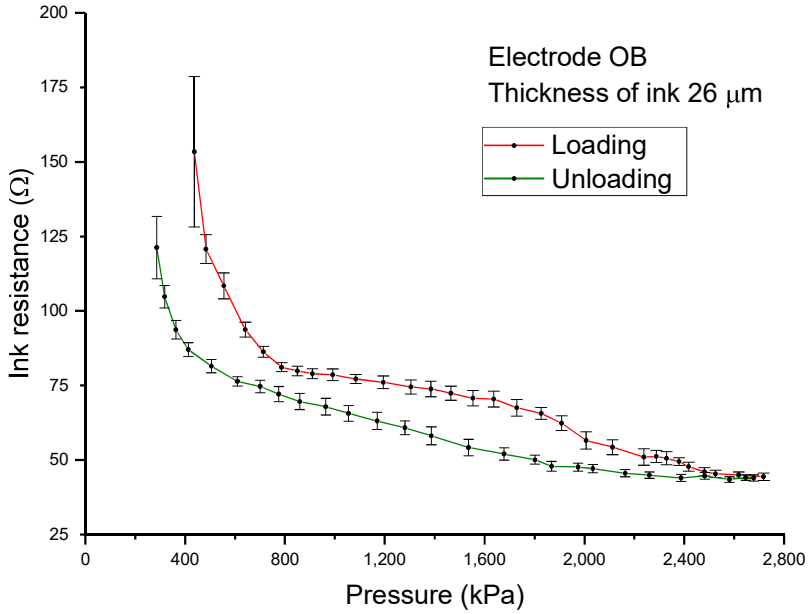

Figure 9. Dependence of measured electrical resistance of a 26 μm thick ink layer on the pressure (loading and unloading cycle).

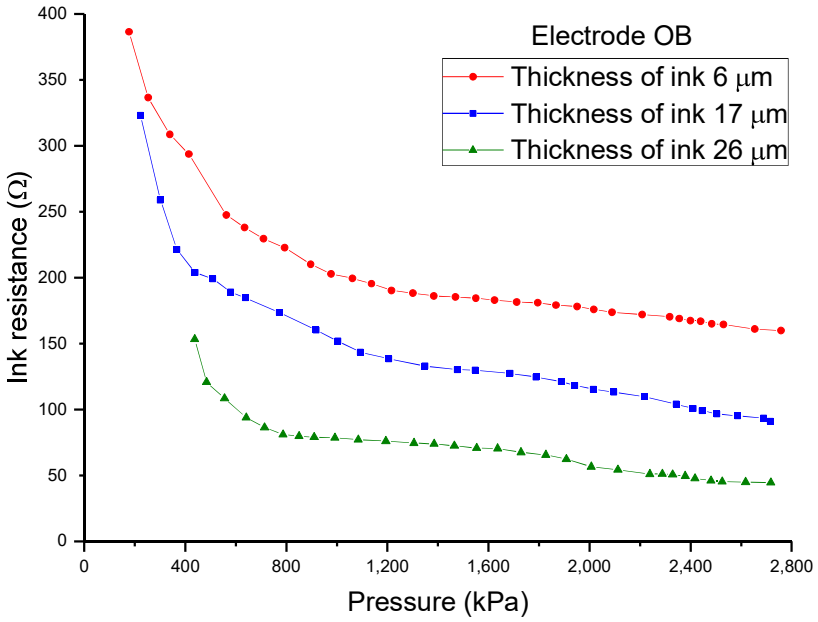

Figure 10. Dependence of measured electrical resistance for 6 μm, 17 μm and 26 μm thick ink layer on the pressure (summary).

All three diagrams exhibit appreciable hysteresis, i.e. a different shape of the curve in the loading and unloading cycle. This may be caused by relaxation of the ink and foil on which the ink is deposited; the hysteresis also limits the possibility to measure the absolute pressure acting on the sensor. From this point of view the 26 μm ink layer seems to be unsuitable due the very different courses of dependency.

By the 6 μm and 17 μm ink layers, the hysteresis is smaller and the lines are rather only vertically shifted unlike the 26 μm layer. Both setups exhibit nearly linear characteristics between 1,000 and 2,400 kPa that meet our initial requirements. It has to be also noted that when increasing the pressure on the measuring point, the C type uncertainty gradually decreases; thus the accuracy of the measurement is better at higher loads where the characteristic is not so steep. Following Fig. 10 summarizes the dependencies for all three ink layers in one graph.

From this graph it is apparent that all curves exhibit sufficient sensitivity in the range from 1,000 to 2,400 kPa, i.e. that the measured resistivity changes significantly with the applied pressure. From this point of view the most suitable seems to be the 17 μm ink layer with slightly steeper course and thus better sensitivity. Out of this range, the sensitivity decreases (above 2,400 kPa; mainly 17 μm and 26 μm layers), or the course does not exhibit the required linear character (cca. below 1,000 kPa, all curves).

We can conclude, that within a given pressure range (1,000–2,400 kPa) the 17 μm ink layer exhibits the best properties to act as converter between pressure and electrical resistance. The main limitations are persistent hysteresis and not entirely linear dependency of the electrical resistance on the pressure. These negatives can be, however, particularly eliminated by post-processing of the raw data using a dedicated computer program. The measurements of resistance with other materials and with other electrode types are discussed in Volf et al. (2012), Volf et al. (2015) and Volf et al. (2016).

CONCLUSIONS

The new developed planar pressure measuring system Plantograf V18 brings some new features and significant improvements: it is capable due to its high refresh rate to capture highly dynamics processes, which is essential e.g. in sports medicine or athlete training. The new developed electronic control circuits enable to change the gain, thus this transducer is capable to measure the pressure under human feet as well as car tyres. Due to its high sensor density and much wider pressure range, it is supposed to measure the pressure distribution under fine tire patterns on all agricultural machines, as well as other large transport means.

There are similar planar measurement systems in the world, for technical details see Texscan, Rsscan or Xsensor (2017). However, these systems have several limitations compared to Plantograf: limited resolution given the dimensions of the electrodes and their density, much lower frame rate and buffer size that limits the scanning time or inability to obtain raw data. Compared to those pressure transducers, this system processes a real-time signal from 16,400 sensors with a frame rate of 500 frames per second; in the future development, this should increase up to 1,000 frames per second. This is enabled by parallel processing of data from individual sensors. This makes this system much faster maintaining its incomparably high resolution due to its dense network.

The measurements with new OB electrode types with 3.5 mm diameter gave satisfactory results. As the transducer between applied pressure and output electrical resistance was selected conductive ink DZT-3K, deposited on a thin foil. Within the pressure range 1,000–2,400 kPa, the 17 μm ink layer exhibited nearly linear characteristic of dependency as required, as well as relatively small hysteresis and sufficient sensitivity, compared to other configurations with different ink layer thicknesses.

ACKNOWLEDGEMENTS. The measurements were carried out within the IGA project of the Faculty of Engineering, Czech University of Life Sciences in Prague.

REFERENCES

Astellanos-Ramos, J. & Navas-Gonzáles, R. 2010. Tactile sensors based on conductive polymers. *Microsystem Technologies* **16**, 765–776.

Dahiya, R. & Valle, M. 2008. *Sensors: Focus on Tactile Force and Stress Sensors*.

Fraden, J. 2010. *Handbook of modern sensors: physics, designs, and applications*. New York, Springer, 2010, 663 pp. ISBN 978-1-4419-6465-6.

Kim, K. 2009. Polymer-based flexible tactile sensor up to 32×32 arrays integrated with interconnection terminals. *Sensors and Actuators A: Physical* **156**, 284–291.

Lee, M.H. 2000. Tactile sensing: New directions, new challenges. *The International Journal of Robotics Research* **19**, 636–643.

Seminara, L., Pinna, L., Valle, M., Basiricò, L., Loi, A., Cosseddu, P., Bonfiglio, A., Ascia, A., Biso, M., Ansaldo, A., Ricci, D. & Metta, G. 2013. Piezoelectric Polymer Transducer Arrays for Flexible Tactile Sensors. *IEEE Sensors Journal* **13**, 4022–4029.

Tekscan. *http://www.tekscan.com.* Accessed 10.12.2017.

Volf, J., Trinkl, A., Novák, M., Bílek, J., Prikner, P. & Neuberger, P. 2012. Plantograf V12 with Optimal Size Determination Sensor Electrodes and its Using for Pressure Distribution Between Tire and Road. In: *XX World Congress IMEKO*. IMEKO, Busan.

Volf, J., Novák, V. & Ryzhenko, V. 2015. Effect of conductive ink properties of tactile sensors. *Procedia Engineering* **120**, 200–205.

Volf, J., Svatoš, J., Koder, P., Novák, V., Papežová, S., Ryzhenko, V. & Hurtečák, J. 2015. Pressure Distribution Measurement System PLANTOGRAF V12 and its Electrodes Configuration. *Agronomy Research* **13**, 732–738.

Volf, J., Novák, V. & Ryzhenko, V. 2016. Effect of Conductive Ink on Transfer Characteristics of Pressure into Electric Signal for Tactile Sensors. *Agronomy Research* **14**, 1123–1129.

Weiss, K. & Worn, H. 2005. The working principle of resistive tactile sensor cells. In: *IEEE International Conference on Mechatronics and Automations*, 471–476.

Xsensor. *http://www.xsensor.com.* Accessed 10.12.2017.